Why building damage concentrated to Longtoushan Town during the Ms6.5 Ludian Earthquake*

Xin Wang (IRIDeS, Tohoku University), Susumu Kurahashi, Hao Wu (Aichi Institute of Technology), Hongjun Si (ERI, University of Tokyo), Ji Dang (Saitama University), and Kojiro Irikura (DPREC, AIT)

1. INTRODUCTION

An earthquake struck Ludian County, Yunnan, China at 08:30:10.2 UTC (16:30:10.2 local time) on 3 August 2014 with the magnitude M_s6.5 (M_w6.2 by US Geological Survey) and focal depth of 12 km by the China Earthquake Network Center. Though it is a moderate earthquake, it caused unexpected building damage and loss of lives (G. Zhang et al., 2014; L. Xu et al., 2014; Liu et al., 2014; Y. Zhang et al., 2014; Hu et al., 2015; Lin et al., 2015; X. Li, 2015; Xie et al., 2015). As of 8 August, 617 people died, 112 people went missing and a lot of buildings were destroyed (Wang et al., 2014; Cheng et al., 2015). The highest peak ground acceleration (PGA) reached to 949 gal in the E-W component at the Longtoushan seismic station (53LLT), which located at the outskirt of Longtoushan Town and about 8.3 km far from the epicenter (Cheng et al., 2015). Most of the deaths and damaged buildings were concentrated to the Longtoushan Town (Lin et al., 2015; X. Li et al., 2014; X. Li et al., 2015; X. Xu, Chong, et al., 2015), mostly due to building damage and partly to earthquake-induced landslides. (Li et al., 2014; Li et al., 2015; Xu et al., 2015; Lin et al., 2015).

In this paper, the reasons of building damage concentration to the Longtoushan Town are studied comprehensively, combing the generation mechanism of high acceleration at the Longtoushan Town, the ground motion simulation at the proluvial fan and the river terraces considering the different site amplifications which are evaluated using the inversed ground structure based on the microtremor measurement. The vulnerability of the buildings at Longtoushan Town is compared with the 2008 Wenchuan earthquake based on the vulnerability function of the 2008 Wenchuan earthquake (Wang et al., 2011).

2. BUILDING DAMAGE INVESTIGATION

We performed a filed investigation around strong motion stations near the epicenter in the northeast (Longtoushan, Ciyuan, and Zhaotong seismic station) and southwest (Mashu and Qianchang seismic station) direction of the epicenter. Through the investigation, we found masonry buildings are widely used in the disaster area, which is similar to the struck area of 2008 Wenchuan earthquake (Wang et al., 2011). Furthermore, buildings around Longtoushan station suffered serious damage, whereas slight damage around other stations. Almost no building damage happened in the Zhaotong City. Some slight damages, such as cracks in the masonry walls and deformation of foundations, happened in the Ciyuan Town, Qianchang Town and Mashu Town. Severe building damage and building collapse only can be seen in the Longtoushan Town. A remote sensing photo of the severely damaged area (on proluvial fan) in the Longtoushan town is shown in Photo 1. From the photo 1 we can see

*2014 年中国雲南省昭通地震（Ms6.5）における建物被害が龍頭山鎮に集中した原因分析

that on the proluvial fan most of the buildings were collapsed, only rubbles were remained. The building collapse ratio, which is defined as the ratio of partially and totally damaged building, is almost 90 %. Photos of three damaged multistory masonry buildings are shown in the Photo 2, which are counted in to the collapse ratios. Though poor quality of some residential buildings result in severe damage, some buildings built based on the new design codes still failed to achieve the design target (Lin et al., 2015). The direct reasons for building damage should be contributed to be the vulnerability of buildings and the characteristics of input ground motions.

Photo 1. Remote sensing photo of the serverly damaged area of Longtoushan Town

Building-A Building-B Building-C

Photo 2. Typical damage of mutistory masonry buildings (locations are shown in Photo 1)

3. FOCAL MECHANISMS SOLUTION AND RUPTURE PROCESS

As shown in Figure 1 the observed acceleration waveforms at the Longtoushan Station (53LLT) have two impulsive waves. Firstly, we examine the arrival direction of seismic waves based on the particle motion diagrams of P-wave parts and the two impulsive waves. It can be seen that the horizontal plane oscillation of the P-wave part is generally in northwest-southeast direction. Therefore, the azimuth of the starting point of the fault rupture can be assumed to be northwest-southeast direction. The particle motion diagrams of the first and second pulse of the S-wave oscillate are in northwest-southeast and northeast-southwest direction, respectively.

These impulsive waves were considered to be generated from the strong motion generation areas (SMGAs) based on our previous studies on source model studies (e.g. Kurahashi and Irikura, 2010). In order to make clear the mechanism of the generation of large acceleration at Longtoushan Station, we try to construct a short-period source model consisting of strong motion generation areas

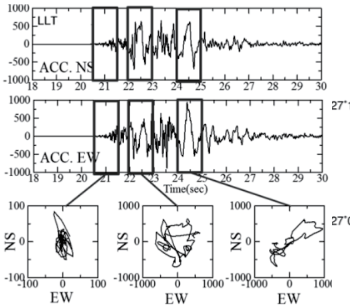

Fig. 1 Particle motions diagrams of waves at 53LLT station

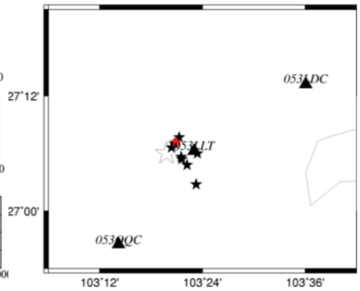

Fig. 2 Source locations of aftershocks with magnitude of greater than 3.7

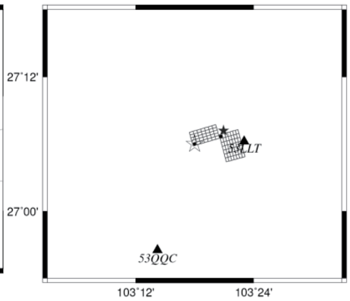

Fig. 3 Short-period source model with two SMGAs (rectangles).

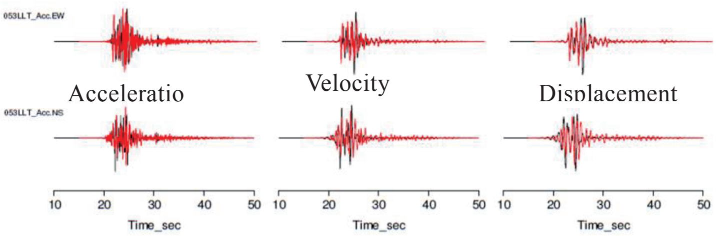

Fig. 4 The comparison between observed (black line) and synthesized (red line) acceleration, velocity and displacement waveforms at 53LLT station. (Bandpass filter 1.0-10Hz)

using the empirical Green's function method (EGFM) (Irikura, et al., 1986). In this source model, we consider both of the conjugate fault planes as source fault. The locations of SMGAs were determined from the aftershock distribution and the particle motion diagrams of the impulsive waves at 53LLT. As a result, the location of SMGA1 for the first impulsive wave was determined on the Baogunao fault. That of SMGA2 for the second one was determined on the Xiaohe fault. We selected the empirical Green's functions from observed records of some aftershocks with magnitude greater than 3.7. Hypocenters of these aftershocks are shown in the Figure 2 with closed star makers. We select one aftershock, whose location is shown with closed red star in Figure 2, to be the empirical Green's function (EGF).

Two SMGAs of the source model are shown in Figure 3. The area and stress drop of each SMGA were about 20km^2 and about 15MPa, respectively. The comparison between observed and synthesized acceleration, velocity, and displacement waveforms in the EW and NS directions at 53LLT station are shown in Figure 4. It can be seen that the synthetic ground motions explain well the characteristics of observed ground motions for either plane.

4. DIFFERENCES OF SITE EFFECTS AT LONGTOUSHAN TOWN

In order to examine the relationship between the site-effects and the building damage on the proluvial fan and the river terrace within the Longtoushan Town, the ground structure of three sites (a01, a02 and, a03, shown in Photo 1) locating from the proluvial fan to the river terrace are reversed using the ground ambient noise. The measurement duration at each site is 30 minutes. To avoid the influence of accidental noises, the thirty-minute data is divided into several tens of windows with length of 20.48 s. Fourier spectra of all windows are stacked. Microtremor H/V spectral ratio, is calculated as the square root of the ratio between horizontal to vertical power spectrum as expressed in equation (1).

$$\frac{H}{V}(f)=\sqrt{\frac{P_{NS}(f)+P_{EW}(f)}{P_{UD}(f)}} \qquad (1)$$

where, $P_{NS}(w)$, $P_{EW}(w)$, and $P_{UD}(w)$ are the power spectrum of microtremor records in the NS, EW, and vertical direction, respectively. One dimensional (1D) underground velocity structures at Longtoushan Station and the three sites a01, a02 and a03 are identified by minimizing the misfit function, Function (2), which expresses the difference between the observed and the theoretical H/V spectral ratios.

$$E_m=\frac{\sum_{f_{\min}}^{f_{\max}}\left|(H/V)^{theo}-(H/V)^{obs}\right|/f_i}{\sqrt{\sum_{f_{\min}}^{f_{\max}}(H/V)^{theo}/f_i}\sqrt{\sum_{f_{\min}}^{f_{\max}}(H/V)^{obs}/f_i}} \qquad (2)$$

where, $(H/V)^{theo}$ and $(H/V)^{obs}$ represent theoretical and observed H/V spectral ratio, respectively.

In order to clarify the ground motion characteristics at the sites (a01-a03) near the strong-motion station, we attempt to estimate the ground motions there using the methodology shown in Figure 5. The estimated PGAs of these three sites are 779 gal (EW), 1101 gal (EW), and 660 gal (NS), respectively, as shown in Figure 6. Considering the predominant periods of microtremor H/V spectral ratios, the predominant periods at heavily damaged sites (a01 and a02) are 0.25 s which is close to the natural period of masonry buildings. While the predominant periods at lightly damaged site (a03) is about 0.15 s.

5. VULBERABILITY OF DAMAGED BUILDINGS

Most of the buildings around the Longtoushan station were public buildings, and were constructed based on seismic design code. Trough field investigation, it can be known that Longtoushan County, most of the buildings were severely damaged or destroyed, including the aseismic buildings. Severe damage or complete collapse of the first story (Lin et al., 2015). Actual earthquake load significantly surpassed intensity 9 (PGA=620 gal). It makes sense that the buildings were all severely damaged. This region was devastated and almost completely covered by debris of buildings Building collapse ratio of this region is estimated to be 95%. The observed building collapse ratios (CRs) are shown in Figure 7. The estimated building collapse ratios of sites a01 to a03 based on the vulnerability curve of the 2008 Wenchuan Earthquake3) are 70%, 85% and 60%, respectively, which are almost 10% greater than the observed ones.

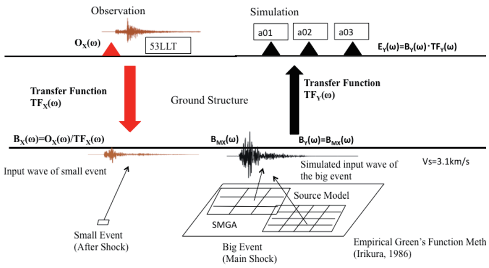

Fig. 5 Method to estimate the ground motions at sites a01-a03 using the ground motion records at the strong-motion station (53LLT)

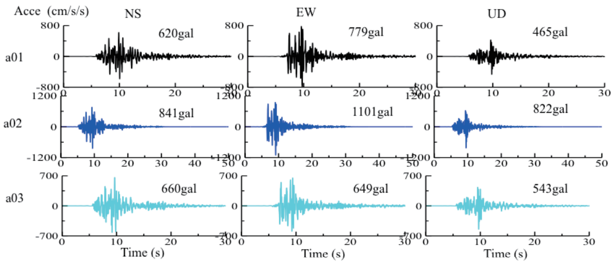

Fig. 6 Estimated acceleration waveforms at the sites a01 (black), a02 (blue) and a03

Fig. 7 observed building collapse ratios (CRs) around the sites a01, a02, and a03

6. CONCLUSIONS

Masonry buildings were very common in attracted areas and severely damaged in Longtoushan Town during this earthquake. Reasons of building damage concentration in the Longtoushan Town during the 2014 Ludian Earthquake are comprehensively examined. The direct reasons for building damage are considered as the high level of ground motions and the vulnerability of buildings. Source characteristics (which relate to the generation of ground motions) and the site effect can be considered as the indirect reasons. The following conclusions can be summarized.

1. Two impulsive waves can be seen on the acceleration waveforms in the Longtoushan Station. A source model including two fault planes is constructed. The generation of large ground motion in Longtoushan Town can be concluded as that it located on the direction of directivity pulses of the source faults.

2. Ground motions were amplified in the high frequency range which includes the frequencies of buildings in Longtoushan Town, which are lowrise masonry buildings. Predominant periods at heavily damaged sites are 0.25 s which is close to the natural period of masonry buildings. While the predominant periods at lightly damaged site is about 0.15 s.
3. Observed CRs of Longtoushan Town are higher than the inferred ones. That is to say the aseismic capacities of masonry buildings should be improved or some other structural types with higher aseismic capacity should be used, such as reinforced concrete buildings, if the economic situation permits.

REFERENCE

Cheng, J., Z. Wu, J. Liu, C. Jiang, X. Xu, L. Fang, X. Zhao,W. Feng, R. Liu, J. Liang, et al. (2015). Preliminary report on the 3 August 2014, Mw 6:2=Ms 6:5 Ludian, Yunnan-Sichuan border, south-west China, earthquake, *Seismol. Res. Lett*. 86, no. 3, 750–763, doi: 10.1785/0220140208.

Hu J., Q. Zhang, Z. Jiang, L. Xie, and B. Zhou (2015), Characteristics of strong ground motions in the 2014 M_s6.5 Ludian earthquake, Yunnan, China, *J. Seismol,* doi:10.1007/s10950-015-9532-x. (in press)

Irikura K. (1986) Prediction of strong acceleration motions using empirical Green's function, Proc. *7th Japan Earthq. Eng. Symp.*, 1986, pp.151-156.

Kurahashi, S. and K. Irikura (2010), Characterized Source Model for Simulating Strong Ground Motions during the 2008 Wenchuan Earthquake, *Bull. Seismol. Soc. Am.*, **100**, pp.2450–2475.

Li X., J. Zhang, Y. Xie, and Q. Miao (2014). Ludian Ms 6.5 earthquake surface damage and its relationship with structure, *Seismol. Geol*. 36, no. 4, 1280–1291 (in Chinese with English abstract).

Li X., X. Xu, Y. Ran, J. Cui, Y. Xie, and F. Xu (2015). Compound fault rupture in the 2014 Ms 6.5 Ludian, China, earthquake and significance to disaster mitigation, *Seismol. Res. Lett*. 86, no. 3, 764–774.

Lin X., H. Zhang, H. F. Chen, H. Chen, and J. Lin (2015), Field investigation on severely damaged aseismic buildings in 2014 Ludian earthquake, *Earth. Eng. & Eng. Vib*. **14,** no.1, 169-176.

Liu, C.,Y. Zheng, X. Xiong, R. Fu, B. Shan, and F. Diao (2014). Rupture process of Ms 6.5 Ludian earthquake constrained by regional broadband seismograms, *Chin. J. Geophys*. 57, 3028–3037, doi: 10.6038/cjg20140927 (in Chinese with English abstract).

Wang, W., J. Wu, L. Fang, and G. Lai (2014). Double difference location of the Ludian Ms 6.5 earthquake sequence in Yunnan Province in 2014, *Chin. J. Geophys*. 57, no. 9, 3042–3051, doi: 10.6038/cjg20140929 (in Chinese with English abstract).

Wang X., K. Masaki, and K. Irikura (2011). Building Damage Criteria from Strong Ground Motion Characteristics during the 2008 Wenchuan Earthquake, *Journal of Earthquake Engineering*, 15:1117-1137.

Xie, Z., Y. Zheng, C. Liu, X. Xiong, Y. Li, and X. Zheng (2015). Source parameters of the 2014 Ms 6.5 Ludian earthquake sequence and their implications on the seismogenic structure, *Seismol. Res. Lett*. 86, no. 6, doi: 10.1785/0220150085.

Xu L., X. Zhang, C. Yang, and C. Li (2014). Analysis of the Love waves for the source complexity of the Ludian M_s 6.5 earthquake, *Chin. J. Geophys*. 57, 3006-3017, doi:10.6038/cjg20140925 (in Chinese with English abstract).

Zhang G., J. Lei, S. Liang, and C. Sun (2014). Relocations and focal mechanism solutions of the 3 August 2014 Ludian, Yunnan M_s6.5 earthquake sequence, *Chin. J. Geophys* **59,** no. 9, 3018-3027. (in Chinese with English abstract)

Zhang Y., L. Xu, Y. Chen, and R. Liu (2014). Rupture process of the 3 August 2014 Ludian, Yunnan, Mw 6.1(Ms 6.5) earthquake, *Chin. J. Geophys*. 57, 3052–3059, doi: 10.6038/cjg20140930 (in Chinese with English abstract).